AGU PUBLICATIONS

Geophysical Research Letters

Supporting Information for

Robust longitudinally-variable responses of the ITCZ to a myriad of climate forcings

Alyssa R. Atwood[1], Aaron Donohoe[2], David S. Battisti[3], Xiaojuan Liu[3], Francesco S.R. Pausata[4]

[1]Department of Earth Ocean and Atmospheric Science, Florida State University, Tallahassee, FL, USA; [2]Polar Science Center, Applied Physics Laboratory, University of Washington, Seattle, Washington 98195, USA; [3]Department of Atmospheric Sciences, University of Washington, Seattle, WA 98195, USA; [4]Centre ESCER (Étude et la Simulation du Climat à l'Échelle Régionale) and GEOTOP (Research Center on the dynamics of the Earth System), Department of Earth and Atmospheric Sciences, University of Quebec in Montreal, Montreal, QC, Canada

Contents of this file

Text S1. Description of surface heat flux correction in CESM

In a 13-year simulation with raised topography over Central America, sea surface temperatures (SSTs) were nudged to observed climatology (NOAA ERSST v3b from 1970-2009) within 30° of the equator (linearly decreasing to zero between 25° and 30° latitude), using a Newtonian cooling in the top layer of the ocean model with a restoring time-scale (τ) of 10 days. The monthly climatology of the surface heat flux adjustment was calculated over the last 10 years of this simulation and applied as a constant (seasonally-varying) surface heat flux adjustment to the final 500-yr control simulation. These bias corrections are applied to both the climatological and perturbed simulations and allow a realistic tropical mean state while simultaneously allowing the tropics to respond in the forced experiments. The tropical surface temperature, precipitation, and wind fields before and after these bias corrections are shown in Figs. S1 and S2. See Atwood (2015) for further information and analysis of these simulations.

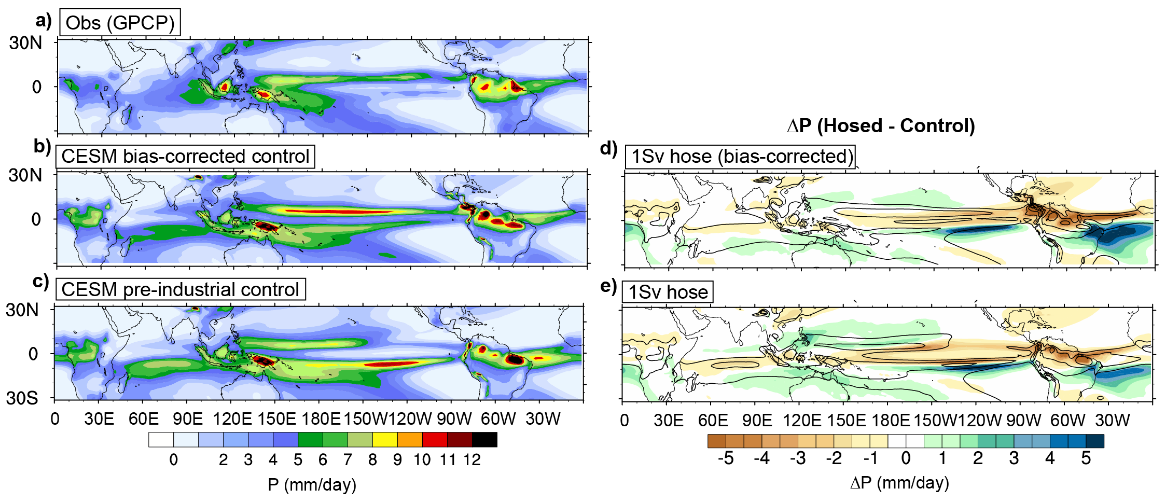

Fig. S1. Left panels: climatology of tropical precipitation in March-April-May (MAM) in (a) observations (GPCP), (b) CESM with surface heat flux corrections and raised central American topography, and (c) the pre-industrial control of CESM. Right panels: ensemble-mean change in MAM precipitation (colors) due to North Atlantic meltwater forcing where the forcing is applied to (d) the bias-corrected CESM control run, and (e) the pre-industrial CESM control run. The climatological ensemble mean precipitation is shown by the unfilled contours (contours = 4, 8, 12 mm/day).

Fig. S1. Left panels: climatology of tropical precipitation in March-April-May (MAM) in (a) observations (GPCP), (b) CESM with surface heat flux corrections and raised central American topography, and (c) the pre-industrial control of CESM. Right panels: ensemble-mean change in MAM precipitation (colors) due to North Atlantic meltwater forcing where the forcing is applied to (d) the bias-corrected CESM control run, and (e) the pre-industrial CESM control run. The climatological ensemble mean precipitation is shown by the unfilled contours (contours = 4, 8, 12 mm/day).

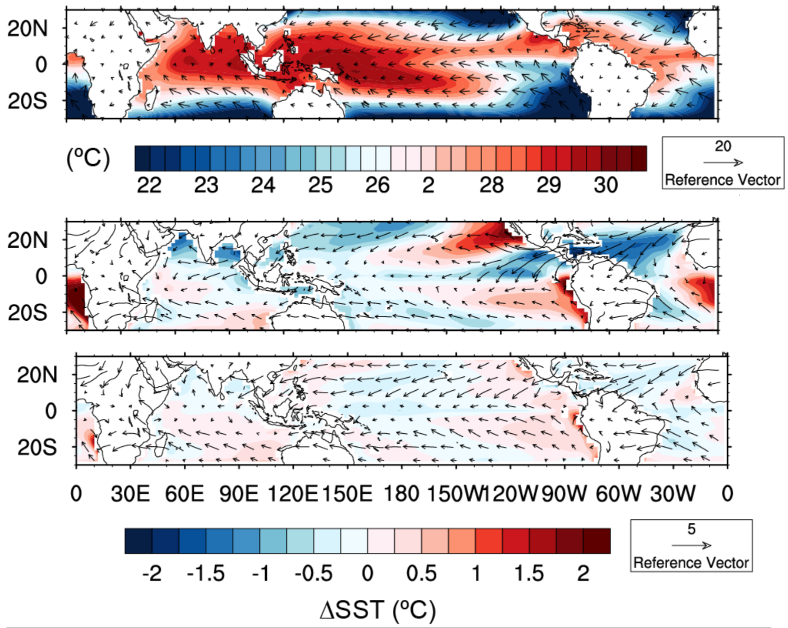

Fig. S2. Observed mean annual climatology of SST and surface winds in ERSST v3b reanalysis (top). SST and surface wind field biases in CESM without (middle) and with (bottom) surface heat flux and central American topography corrections. Note that the magnitude of the reference vector in the top panel is larger by a factor of 4.

Fig. S2. Observed mean annual climatology of SST and surface winds in ERSST v3b reanalysis (top). SST and surface wind field biases in CESM without (middle) and with (bottom) surface heat flux and central American topography corrections. Note that the magnitude of the reference vector in the top panel is larger by a factor of 4.

Table S1. Description of model simulations used in this analysis.

Forcing	Model	Institution	Atm Resolution (lat x lon grid points or spectral, vertical levels)	Ocean Resolution (lat x lon grid points or spectral, vertical levels)	Volcanic forcing details	Reference
Mid-Holocene (PMIP3)	BCC-CSM1.1	Beijing Climate Center, China Meterological Administration, China	T42, L26	232 x 360, L40		Xin et al. (2013)
	CCSM4	National Center for Atmospheric Research, US	0.98° x 1.258°, L26	384 x 320, L60		Gent et al. (2011)
	CNRM-CM5	Center National de Recherches Météorologiques, France	T127, L31	292 x 362, L42		Voldoire et al. (2013)
	CSIRO-Mk3L.1.2	University of New South Wales, Sydney,	T63, L18	189 x 192, L31		Rotstayn et al. (2010)
	FGOALS-g2	LASG, Institute of Atmospheric Physics, Chinese Academy of Sciences; Center for Earth System Science, Tsinghua University, China	60 x 128, L26	196 x 360, L30		Li et al. (2013)
	FGOALS-s2	LASG, Institute of Atmospheric Physics, Chinese Academy of Sciences, China	T42, L26	196 x 360, L30		Bao et al. (2013)
	GISS-E2-R	NASA Goddard Institute for Space Studies, US	2° x 2.5°, L20	180 x 288, L32		Schmidt et al. (2006); Schmidt et al. (2014)
	MIROC-ESM	Japan Agency for Marine-Earth Science and Technology, Atmosphere and Ocean Research Institute (The University of Tokyo), and National Institute for Environmental Studies, Japan	T42, L80	192 x 256, L44		Watanabe et al. (2011)
	MPI-ESM-P	Max Planck Institute for Meteorology, Germany	T63, L47	220 x 256, L40		Raddatz et al. (2007); Marsland et al. (2003)
	MRI-CGCM3	Meteorology Research Institute, Japan	T159, L48	368 x 360, L51		Yukimoto et al. (2012)
4xCO2 (CMIP5)	FGOALS-g2	LASG, Institute of Atmospheric Physics, Chinese Academy of Sciences	60 x 128, L26	196 x 360, L30		Taylor et al. (2012)
	GISS-E2-R	NASA Goddard Institute for Space Studies, US	2° x 2.5°, L40	180 x 288, L32		Schmidt et al. (2014)
	ACESS1.0	Commonwealth Scientific and Industrial	192 x 144, L17	0.6° x 1.0°, L36		Taylor et al. (2012)
	BCC-CSM1	Bjerknes Centre for Climate Research,	64 x 128, L17	232 x 360, L40		"
	CAN ESM2	Canadian Centre for Climate Modelling and	64 x 128, L22	1.9° x 1.9°, L29		"
	NCAR CCSM4	National Center for Atmospheric Research,	288 x 192, L26	320 x 384, L60		"
	CNRM-CM5	Centre National de Recherches Meteorologiques and Centre Europeen de Recherche et Fromation Avancees en Calcul Scientifiqu	256 x 128, L31	292 x 362, L42		"
	CSIRO-Mk3.0	Commonwealth Scientific and Industrial	T63 L18	1.875° x 0.925°, L31		"
	FGOAL S2	LASG, Institute of Atmospheric Physics, Chinese	R42 L226	1.0° x 1.0°, L16		"
	GFDL CM3	NOAA Geophysical Fluid Dynamics Laboratory	C48 L48	360 x 200, L50		"
	GFDL ESM2G	NOAA Geophysical Fluid Dynamics Laboratory	M45 L24	360 x 210, L63		"
	GFDL ESM2M	NOAA Geophysical Fluid Dynamics Laboratory	M45 L24	360 x 200, L50		"
	INMCM4	Institute for Numerical Mathematics	2.0° x 1.5°, L21	2.0° x 0.5°, L40		"
	IPSL CM5A	Institut Pierre-Simon Laplace	96 x 95, L39	2.0° x 2.0°, L31		"
	IPSL CM5B	Institut Pierre-Simon Laplace	96 x 95, L39	2.0° x 2.0°, L31		"
	MIROC5	Atmosphere and Ocean Research Institute (The	T85, L40	256 x 224, L50		"
	MPI ESM	Max Planck Institute for Meteorology	T63, L47	GR15, L40		"
	MRI CGCM3	Meteorological Research Institute	TL159, L48	368 x 360, L51		"
	NorESM1-M	Norwegian Climate Centre	144 x 96, L26	384 x 320, L53		Bentsen et al. (2013); Iversen et al. (2013)
LGM (PMIP3)	CCSM4	National Center for Atmospheric Research, US	192 x 288, L26	320 x 384, L60		Taylor et al. (2012); Harrison et al. (2014)
	CNRM-CM5	Centre National de Recherches Meteorologiques and Centre Europeen de Recherche et Fromation Avancees en Calcul Scientifiqu	128 x 256, L17	292 x 362, L42		"
	GISS-E2-R	NASA Goddard Institute for Space Studies, US	90 x 144, L17	180 x 288, L32		Schmidt et al. (2014)
	MIROC-ESM	Japan Agency for Marine-Earth Science and Technology, Atmosphere and Ocean Research Institute (The University of Tokyo), and National Institute for Environmental Studies, Japan	64 x 128, L35	192 x 256, L44		Taylor et al. (2012); Harrison et al. (2014)
	MPI-ESM-P	Max Planck Institute for Meteorology	96 x 192, L25	220 x 256, L40		"
	MRI-CGCM3	Meteorological Research Institute	160 x 320, L23	368 x 360, L51		"
LGM (PMIP2)	CNRM-CM3.3	Centre National de Recherches Meteorologiques and Centre Europeen de Recherche et Fromation Avancees en Calcul Scientifiqu	128 x 64, L16	182 x 152, L31		Salas-Melia et al. (2005)
	FGOALS- 1.0g	LASG, Institute of Atmospheric Physics, Chinese Academy of Sciences, China	128 x 60, L17	360 x 180, L33		Yu et al. (2002)
	HadCM3	Hadley Centre, Met Office, UK	96 x 72, L15	288 x 144, L20		Gordon et al (2000)
	IPSL - CM4	Institut Pierre-Simon Laplace	96 x 72, L19	180 x 90, L31		Marti et al. (2005)
	MIROC3.2.2	Japan Agency for Marine-Earth Science and Technology, Atmosphere and Ocean Research Institute (The University of Tokyo), and National Institute for Environmental Studies, Japan	T42, L20	1.4° x 0.5°, L43		K-1-Model-Developers (2004)
	ECHAM5 - 5.3	Max-Planck-Institute for Meteorology	T31, L19	1.875° x 0.84°, L40		Roeckner et al. (2003)
	CCSM3	National Center for Atmospheric Research, US	T42 (64 x 128), L26	320 x 384, L40		Otto-Bliesner et al. (2006)
1.0 Sv hosing	CESM 01	National Center for Atmospheric Research, US	288 x 192, L26	320 x 384, L60		Atwood (2015)
	CESM 02	"	"	"		"
	CESM 03	"	"	"		"
	CESM 04	"	"	"		"
	CESM topo 01	"	"	"		"
	CESM topo 02	"	"	"		"
	CESM topo 03	"	"	"		"
	CESM SHF & topo 01	"	"	"		"
	CESM SHF & topo 02	"	"	"		"
	CESM SHF & topo 03	"	"	"		"
	CESM SHF & topo 04	"	"	"		"
	MPI-OM1	Max Planck Institute for Meteorology	T31, L19	3° x 3°, L40		Roeckner et al. (2003), Marsland et al. (2003)
	HadCM3	Hadley Centre, Met Office, UK	2.5° x 3.75°, L19	1.25° x 1.25°, L20		Gordon et al. (2000)
0.1 Sv hosing	CESM SHF & topo 01	National Center for Atmospheric Research, US	192 x 288, L26	384 x 320, L60		Atwood (2015)
	CESM SHF & topo 02	"	"	"		"
	CESM SHF & topo 03	"	"	"		"
	CESM SHF & topo 04	"	"	"		"
NH volcanoes	CCSM4	National Center for Atmospheric Research, US	192 x 288, L26	384 x 320, L60	GRA (sulfate loading)	Landrum et al. (2013)
	GISS 122	NASA Goddard Institute for Space Studies, US	90 x 144, L40	180 x 288, L32	CEA (AOD) x 2	Colose et al. (2016)
	GISS 125	"	90 x 144, L40	180 x 288, L32	CEA (AOD) x 2	"
	GISS 128	"	90 x 144, L40	180 x 288, L32	CEA (AOD) x 2	"
	CESM LME 001	National Center for Atmospheric Research, US	96 x 144, L30	384 x 320, L60	GRA (sulfate loading)	Otto-Bliesner et al. (2016)
	CESM LME 002	"	"	384 x 320, L60	GRA (sulfate loading)	"
	CESM LME 003	"	"	384 x 320, L60	GRA (sulfate loading)	"
	CESM LME 004	"	"	384 x 320, L60	GRA (sulfate loading)	"
	CESM LME 005	"	"	384 x 320, L60	GRA (sulfate loading)	"
	NorESM Laki EM 1-16	Norwegian Climate Centre	96 x 144, L26	384 x 320, L53	Sulfate and dust loading	Bentsen et al. (2013); Iversen et al. (2013)
	NorESM Laki EM 17-3	"	"	"	"	"
	NorESM Laki EM 33-4	"	"	"	"	"
SH volcanoes	CCSM4	National Center for Atmospheric Research, US	192 x 288, L26	384 x 320, L60	GRA (sulfate loading)	Landrum et al. (2013)
	GISS 122	NASA Goddard Institute for Space Studies, US	90 x 144, L40	180 x 288, L32	CEA (AOD) x 2	Colose et al. (2016)
	GISS 125	"	90 x 144, L40	180 x 288, L32	CEA (AOD) x 2	"
	GISS 128	"	90 x 144, L40	180 x 288, L32	CEA (AOD) x 2	"
	CESM LME 001	National Center for Atmospheric Research, US	96 x 144, L30	384 x 320, L60	GRA (sulfate loading)	Otto-Bliesner et al. (2016)
	CESM LME 002	"	"	384 x 320, L60	GRA (sulfate loading)	"
	CESM LME 003	"	"	384 x 320, L60	GRA (sulfate loading)	"
	CESM LME 004	"	"	384 x 320, L60	GRA (sulfate loading)	"
	CESM LME 005	"	"	384 x 320, L60	GRA (sulfate loading)	"

References for Supplementary Material

1. A. R. Atwood (2015) Mechanisms of Tropical Pacific Climate Change During the Holocene." in PhD thesis (University of Washington).
2. X.-G. Xin, T.-W. Wu, J. Zhang, Introduction of CMIP5 experiments carried out with the climate system models of Beijing Climate Center Advances in Climate Change Research 4, 41-49 (2013).
3. P. R. Gent et al., The Community Climate System Model Version 4. J. Clim. 24, 4973-4991 (2011).
4. A. Voldoire et al., The CNRM-CM5.1 global climate model: description and basic evaluation. Clim. Dyn. 40, 2091-2121 (2013).
5. L. D. Rotstayn et al., Improved simulation of Australian climate and ENSO-related rainfall variability in a global climate model with an interactive aerosol treatment. Int. J. Climatol. 30, 1067-1088 (2010).
6. L. Li et al., The flexible global ocean-atmosphere-land system model, Grid-point Version 2: FGOALS-g2. Adv. Atmos. Sci. 30, 543-560 (2013).
7. Q. Bao et al., The Flexible Global Ocean-Atmosphere-Land system model, Spectral Version 2: FGOALS-s2. Adv. Atmos. Sci. 30, 561-576 (2013).
8. G. A. Schmidt et al., Present-day atmospheric simulations using GISS ModelE: comparison to in situ, satellite, and reanalysis data. J. Clim. 19, 153-192 (2006).
9. G. A. Schmidt et al., Configuration and assessment of the GISS ModelE2 contributions to the CMIP5 archive. Journal of Advances in Modeling Earth Systems 6, 141-184 (2014).
10. S. Watanabe et al., MIROC-ESM 2010: model description and basic results of CMIP5-20c3m experiments. Geosci. Model Dev. 4, 845-872 (2011).
11. T. J. Raddatz et al., Will the tropical land biosphere dominate the climate–carbon cycle feedback during the twenty-first century? Clim. Dyn. 29, 565-574 (2007).
12. S. J. Marsland, H. Haak, J. H. Jungclaus, M. Latif, F. Röske, The Max-Planck-Institute global ocean/sea ice model with orthogonal curvilinear coordinates. Ocean Modelling 5, 91-127 (2003).
13. S. Yukimoto et al., A New Global Climate Model of the Meteorological Research Institute: MRI-CGCM3 - Model Description and Basic Performance. Journal of the Meteorological Society of Japan. Ser. II 90A, 23-64 (2012).
14. K. E. Taylor, R. J. Stouffer, G. A. Meehl, An overview of CMIP5 and the experiment design. Bull. Am. Meteorol. Soc. 93, 485-498 (2012).
15. T. Iversen et al., The Norwegian Earth System Model, NorESM1-M – Part 2: Climate response and scenario projections. Geosci. Model Dev. 6, 389-415 (2013).
16. S. P. Harrison et al., Climate model benchmarking with glacial and mid-Holocene climates. Clim. Dyn. 43, 671-688 (2014).
17. D. Salas-Melia et al., Description and validation of the CNRM-CM3 global coupled model. CNRM working note 103 (2005).
18. Y. Yongqiang, Y. Rucong, Z. Xuehong, L. Hailong, A flexible coupled ocean-atmosphere general circulation model. Adv. Atmos. Sci. 19, 169-190 (2002).

19. C. Gordon et al., The simulation of SST, sea ice extents and ocean heat transports in a version of the Hadley Centre coupled model without flux adjustments. Clim. Dyn. 16, 147-168 (2000).
20. O. Marti et al., The new IPSL climate system model: IPSL-CM4. Note du Pôle de Modélisation, IPSL 26, 1-86 (2005).
21. K-1-Model-Developers (2004) K-1 Coupled GCM (MIROC) Description. in K-1 technical report 1, eds H. Hasumi, S. Emori (Center for Climate System Research, University of Tokyo).
22. E. Roeckner et al. (2003) The atmospheric general circulation model ECHAM5—Part I: Model description. in Max-Planck-Institut für Meteorologie, Technical Report.
23. B. L. Otto-Bliesner et al., Last Glacial Maximum and Holocene Climate in CCSM3. J. Clim. 19, 2526-2544 (2006).
24. L. Landrum et al., Last Millennium Climate and Its Variability in CCSM4. J. Clim. 26, 1085-1111 (2013).
25. C. M. Colose, A. N. LeGrande, M. Vuille, Hemispherically asymmetric volcanic forcing of tropical hydroclimate during the last millennium. Earth System Dynamics 7, 681-696 (2016).
26. B. L. Otto-Bliesner, E. C. Brady, J. Fasullo, Climate Variability and Change since 850 CE: An Ensemble Approach with the Community Earth System Model Bull. Am. Meteorol. Soc. 97, 735-754 (2016).